Phosphorylation versus O-GlcNAcylation: Computational Insights into the Differential Influences of the Two Competitive Post-Translational Modifications

Lata Rani and Sairam S. Mallajosyula*

Department of Chemistry, Indian Institute of Technology Gandhinagar, Palaj, Gandhinagar, Gujarat, India - 382355

E-mail: msairam@iitgn.ac.in

Phone: +91 - 79 – 2395 2459

SUPPORTING INFORMATION

Table S1: Dimensions of the water boxes used in the dipeptide simulations.

Dipeptide	**Water box size (Å^3)**
Ser	37×37×37
Thr	37×37×37
SEP	37×37×37
TPO	37×37×37
β-O-GlcNAc (S)	31×31×31
β-O-GlcNAc (T)	31×31×31

Table S2: Dihedral values (ϕ) for the central two residues calculated from the NMR J-coupling data.

	ϕ (C-N-Cα-C)		
Residue	**KSPP**	**KS$_P$PP**	**KS$_{OG}$PP**
S	-82^o	-83^o	-83^o
P	-80^o	-71^o	-77^o
Residue	**KTPP**	**KT$_P$PP**	**KT$_{OG}$PP**
T	-80^o	-82^o	-82^o
P	-87^o	-51^o	-77^o

Table S3: Dimensions of the water boxes used in the model peptide simulations. All sizes are in $Å^3$.

	Unmodified	**Phosphorylated**	**O-GlcNAcylated**
AKAA**A**AKAAAAKAA	56×56×56	---	---
AKAA**S**AKAAAAKAA	55×55×55	55×55×55	110×110×110
AKAA**T**AKAAAAKAA	55×55×55	55×55×55	109×109×109
K**S**PP	47×47×47	44×44×44	48×48×48
K**T**PP	59×59×59	39×39×39	53×53×53

Table S4: $^3J_{\alpha N}$ coupling constants obtained from dipeptide MD simulations.

$^3J_{\alpha N}$	**Experimental**	**Theoretical[d]**
Ser	7.0 Hz[a]	7.7± 1.7 Hz
Thr	7.4 Hz[a]	7.5± 1.7 Hz
SEP	5.9 Hz[b]	6.7± 1.8 Hz
TPO	5.0 Hz[b]	7.2± 1.7 Hz
O-GlcNAc (S)	6.8 Hz[c]	7.2± 3.1 Hz
O-GlcNAc (T)	7.5 Hz[c]	7.5± 2.8 Hz

[a] Experimental $^3J_{\alpha N}$ coupling constants obtained from Ref 68.

[b] Experimental $^3J_{\alpha N}$ coupling constants evaluated at a pH of 8.0 obtained from Ref 58.

[c] Experimental $^3J_{\alpha N}$ coupling constants obtained from Ref 14.

[d] Theoretical coupling constants calculated using the Karplus equations (1) and (2).

Table S5: Percentage populations of the β-sheet and PPII conformations.

Peptide	**Percentage population**	
	β-sheet	**PPII**
KSPP	29.26	65.34
KS_PPP	2.96	84.47
$KS_{OG}PP$	23.13	71.48
KTPP	25.92	69.87
KT_PPP	2.96	84.47
$KT_{OG}PP$	23.13	71.48

Table S6: Distribution of the χ dihedral (N-Cα-Cβ-OG) in the three conformational bins, g+, g- and anti for KTPP, KT_PPP and $KT_{OG}PP$ peptides. The average value of the dihedral in the conformational bins and the associated value of the $J_{H\alpha H\beta}$ coupling constant are also presented.

	g+ (60^0)[a]			**g- (-60^0)[a]**			**anti (180^0)[a]**		
Peptide	**Average**	**Population (%)**	**$J_{H\alpha H\beta}$**	**Average**	**Population (%)**	**$J_{H\alpha H\beta}$**	**Average**	**Population (%)**	**$J_{H\alpha H\beta}$**
KTPP	46.2	45	4.5	-54.8	36	10.0	165.0	19	4.7
KT_PPP	53.0	5	4.6	-47.3	95	9.9	-	-	-
$KT_{OG}PP$	-	-	-	-61.3	83	10.0	150.6	17	5.0

[a] Definition of the conformational bins: g+ ($0^0<\chi<120^0$), g- ($-120^0<\chi<0^0$), anti ($-180^0<\chi<-120^0$ or $120^0<\chi<180^0$)

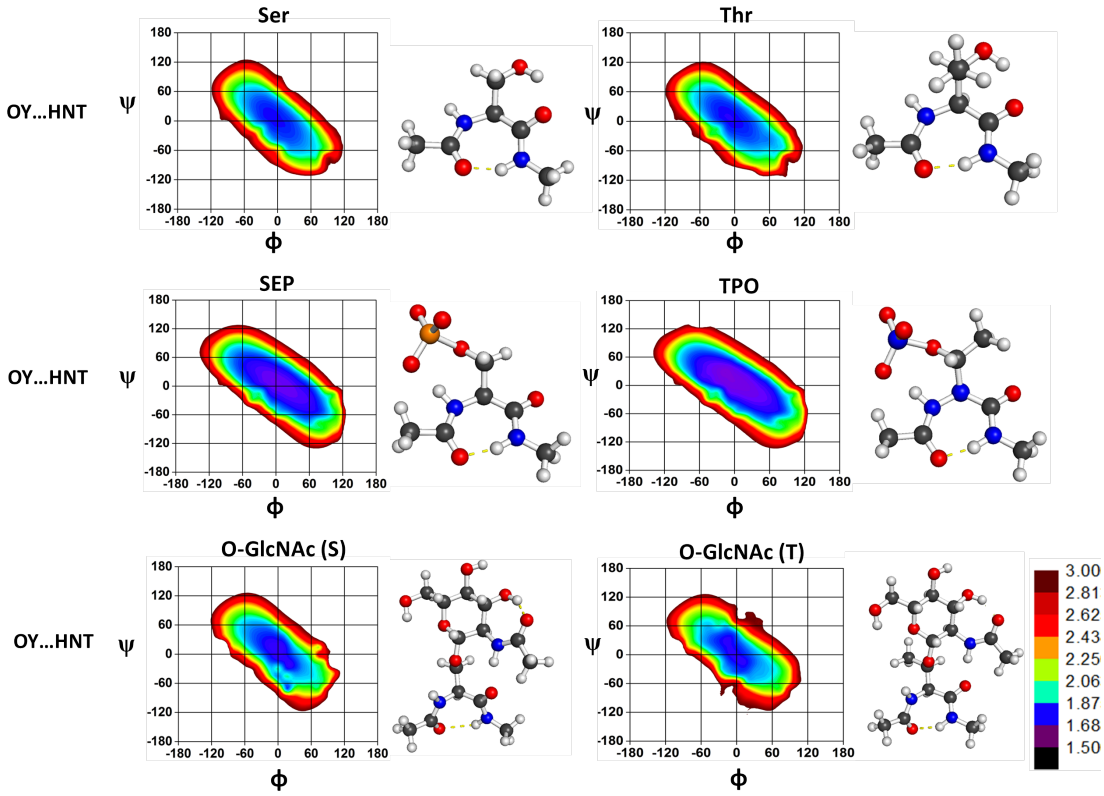

Figure S1: 2D distribution of the OY…HNT H-bond distances as a function of ϕ/ψ dihedrals for all the dipeptides. Structures exhibiting the OY…HNT H-bond have been presented for illustration. The distances are presented in Å, with contours every 0.25 Å. Only distances between the range 1.25 Å - 3.0 Å have been plotted for the sake of clarity.

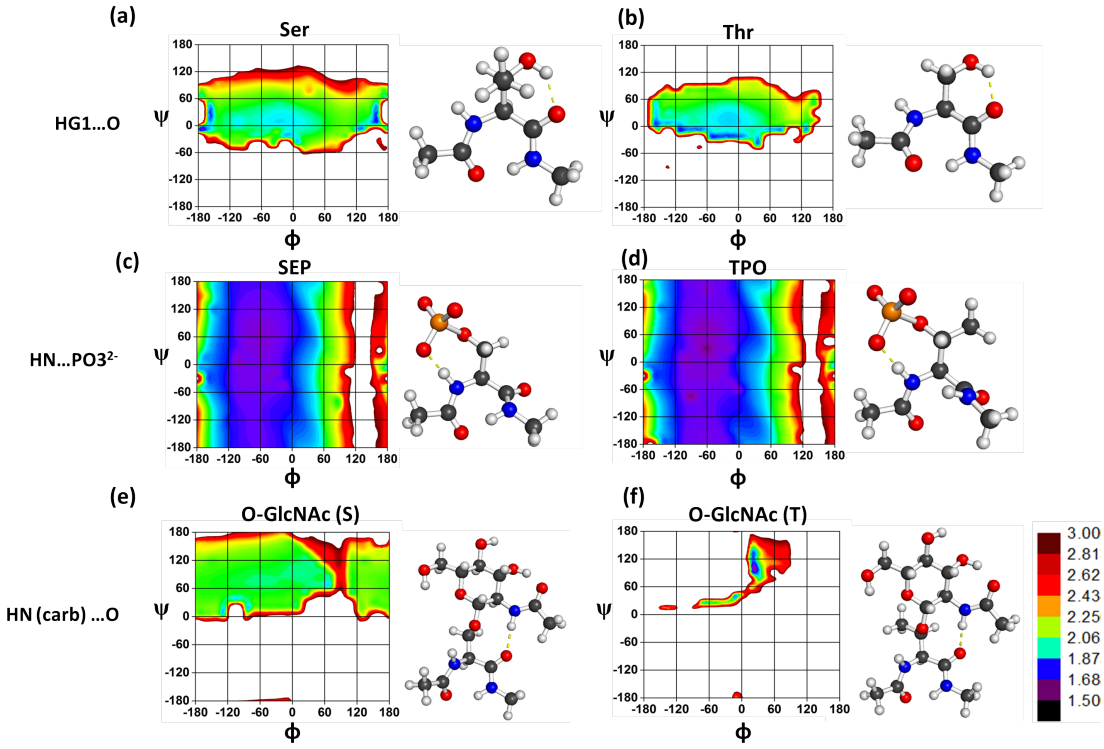

Figure S2: 2D distribution of HG1…O H-bond distances as a function of ϕ/ψ dihedrals for (a) Ser and (b) Thr dipeptides. 2D distribution of HN…OP H-bond distances as a function of ϕ/ψ dihedrals for (c) SEP and (d) TPO dipeptides. 2D distribution of HN_{carb}…O H-bond distances as a function of ϕ/ψ dihedrals for (e) O-GlcNAc (S) and (f) O-GlcNAc (T) dipeptides. Structures exhibiting the described H-bonds have been presented for illustration. The distances are presented in Å, with contours every 0.25 Å. Only distances between the range 1.25 Å - 3.0 Å have been plotted for the sake of clarity.

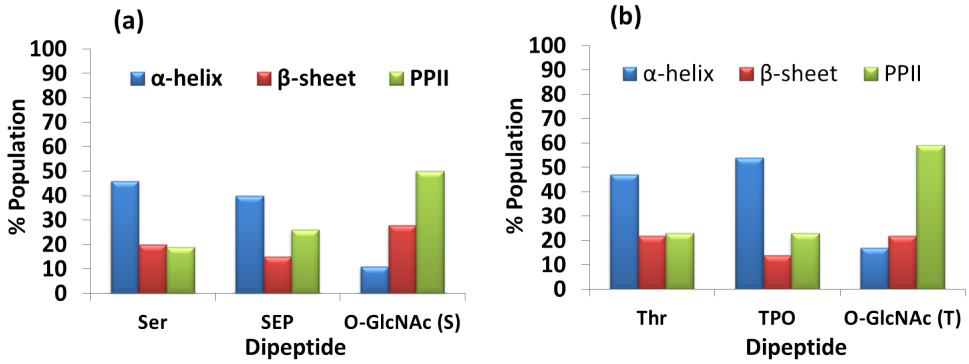

Figure S3: Relative population distributions in the α-helix, β-sheet and PPII-helical regions for (a) Ser/SEP/O-GlcNAc (S) and (b) Thr/TPO/O-GlcNAc (T) from di-peptide MD simulations.

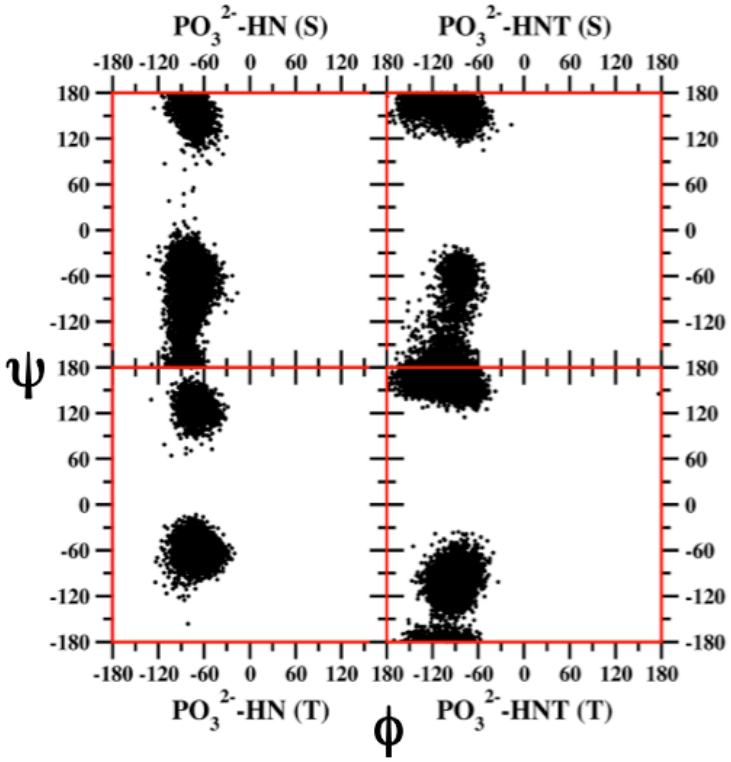

Figure S4: ϕ/ψ distributions corresponding to PO_3-HN and PO_3/HNT H-bonded structures ($d_{H\text{-}bond}$ < 3.0 Å) from SEP and TPO dipeptide simulations.

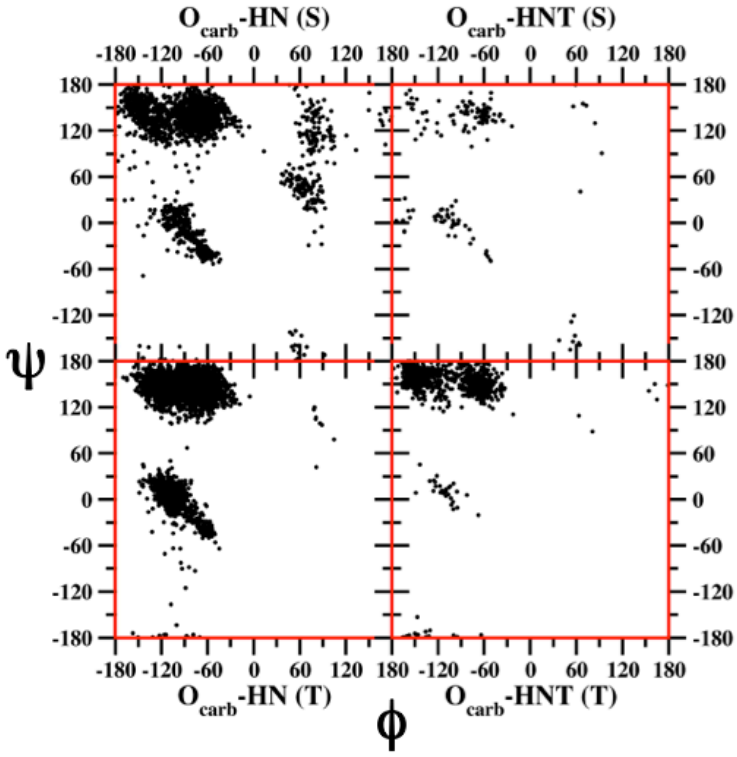

Figure S5: ϕ/ψ distributions corresponding to O_{carb}-HN and O_{carb}-HNT H-bonded structures ($d_{H\text{-}bond}$ < 3.0 Å) from O-GlcNAc (S) and O-GlcNAc (T) dipeptide simulations.

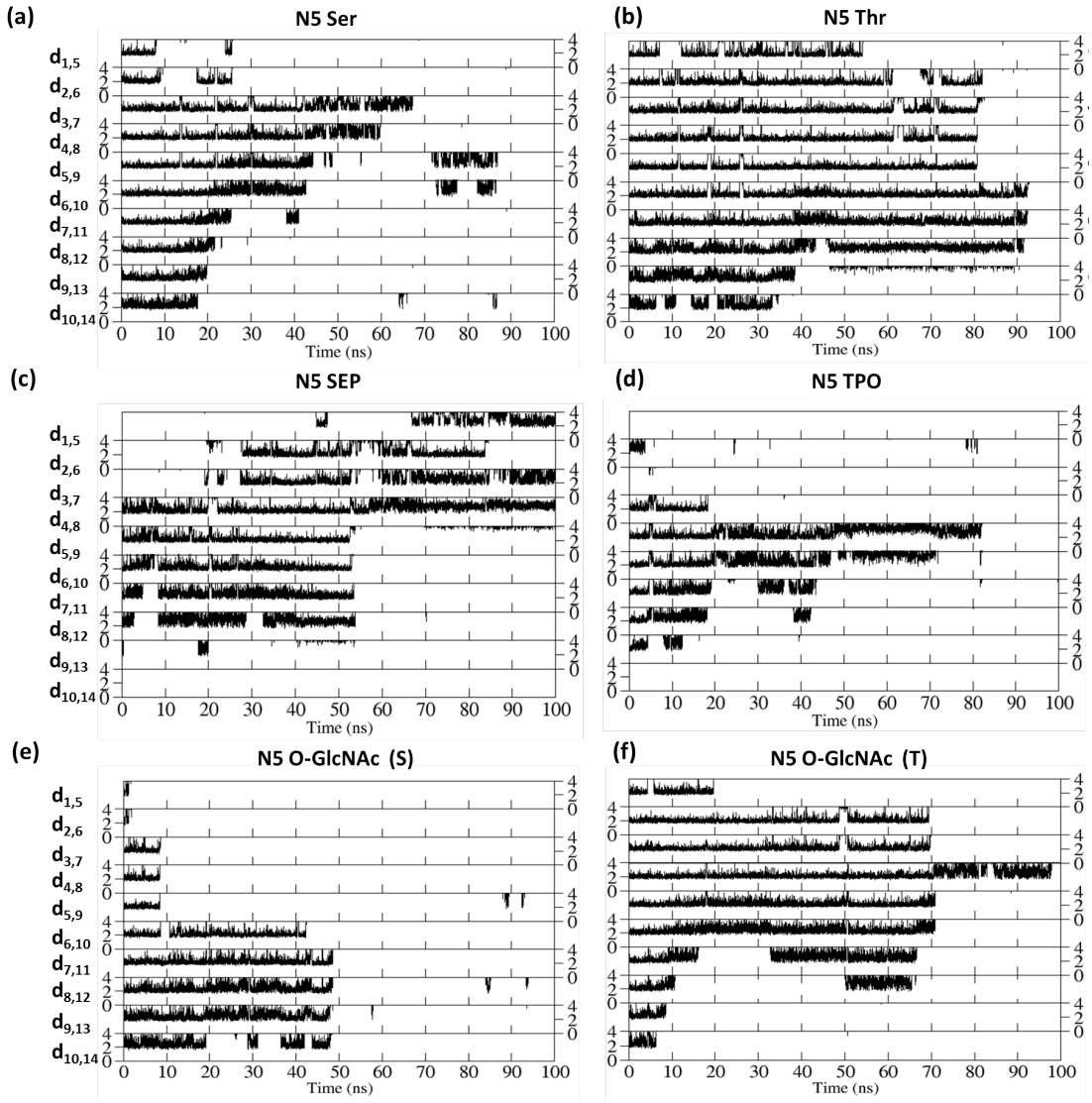

Figure S6: $d_{i,\ i+4}$ backbone O…HN H-bond distances ($d_{H\text{-}bond}$ < 4.0 Å) from the Baldwin peptide simulations. (a) N5 Ser, (b) N5 Thr, (c) N5 SEP, (d) N5 TPO, (e) N5 O-GlcNAc (S) and (f) N5 O-GlcNAc (T). All distances are in Å.

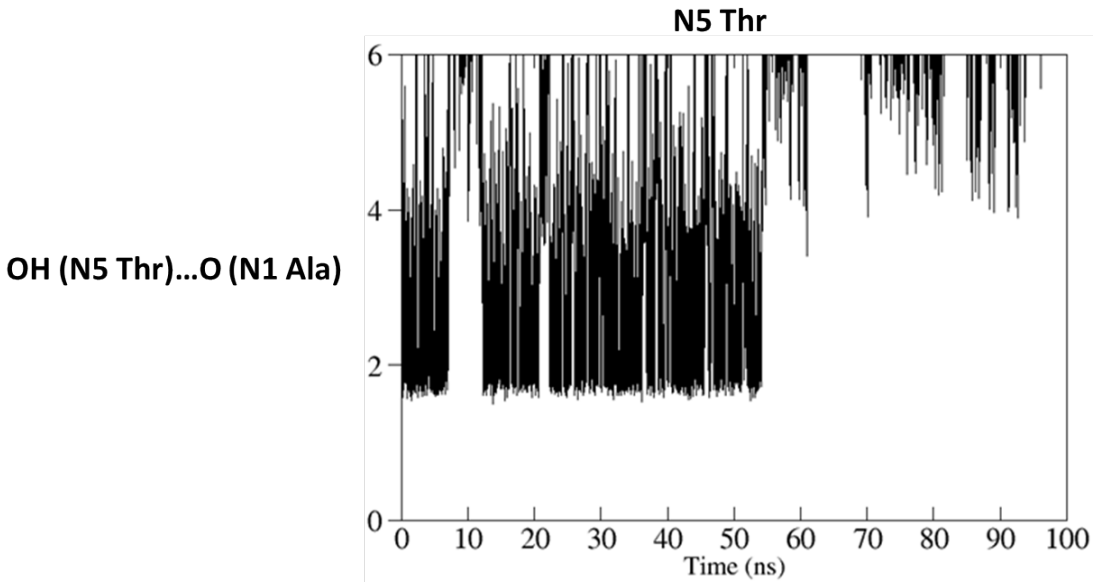

Figure S7: OH (**N5** Thr)…O (**N1** Ala) H-bond distances ($d_{H\text{-}bond}$ < 6.0 Å) from the **N5** Thr Baldwin peptide simulations. Distances are in Å.

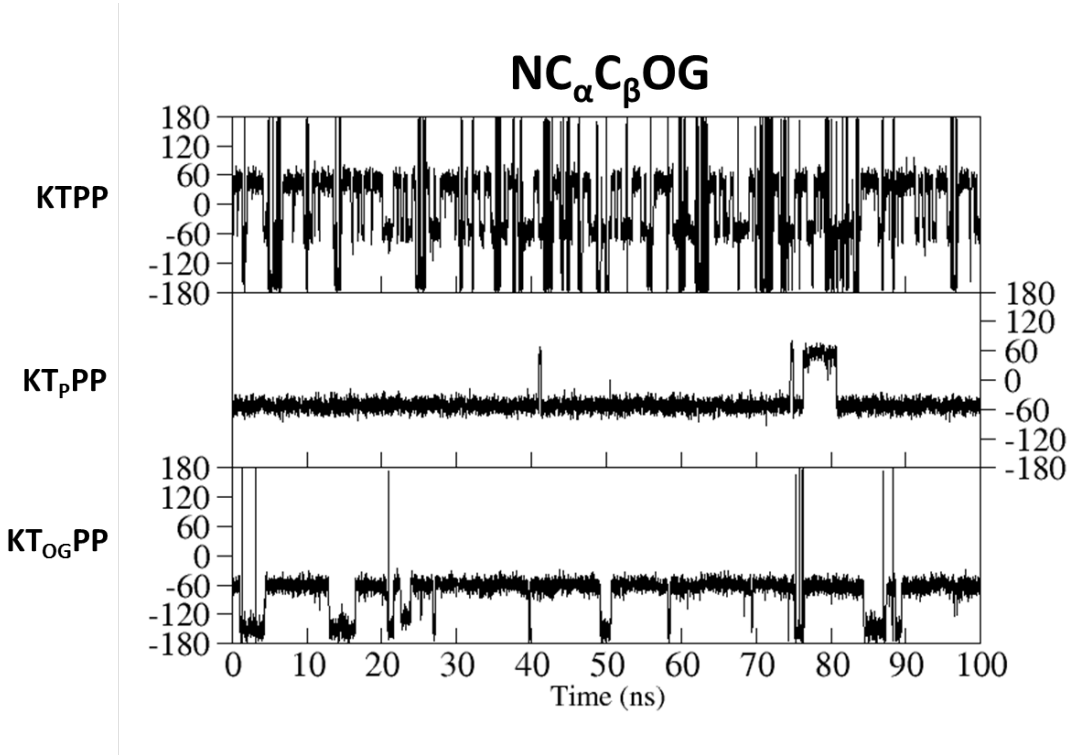

Figure S8: $NC_{\alpha}C_{\beta}OG$ time series corresponding to KTPP, KT_PPP and $KT_{OG}PP$. Dihedral values are reported in ^{0}.

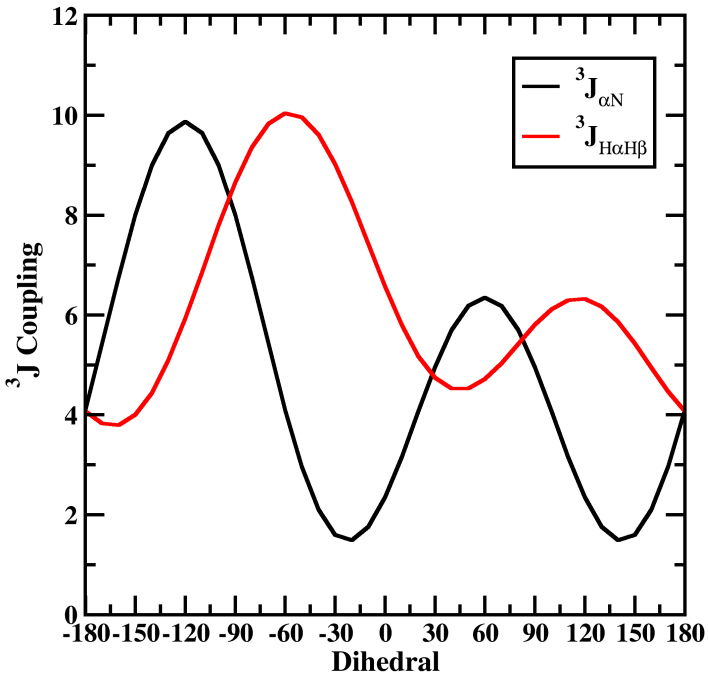

Figure S9: Karplus curves corresponding to the ^{3}J coupling constant as a function of dihedral values evaluated using equation (1) and (2). $^3J_{\alpha N}$ corresponds to the ϕ (C-N-Cα-C) dihedral values while $^3J_{H_\alpha H_\beta}$ correspond to the χ_1 (N-Cα–Cβ–OG) dihedral.